http://dx.doi.org/10.5755/j01.eee.20.5.7061 ELEKTRONIKA IR ELEKTROTECHNIKA, ISSN 1392–1215, VOL. 20, NO. 5, 2014

Driver Topology Influence on LED Luminescence Response Dynamics

A. Chaziachmetovas[1]

[1]*Department of Electronics Engineering, Kaunas University of Technology, Studentu St. 50, LT-51368 Kaunas, Lithuania*

andrius.chaziachmetovas@ktu.lt

***Abstract*—The investigation light-emitting diode (LED) dimming temporal response when used in large scale LED video displays is presented. The aim was to find the response times for several driver topologies. Four driver topologies were considered: commercial constant current driver, passive driver, transconductance amplifier and constant current driver with tamper turn-off. 85 red Screen Master LEDs from Cotco were used in experiments. Measurement setup and circuit diagrams of the equipment used are presented. Measurement results for rise and fall fronts measurement are reported. Investigation results indicate that circuits possessing fast constant current drive (passive driver, transconductance amplifier and constant current driver with tamper turn-off) have similar performance for the front where this constant current source is operational: rise time. Average rise time for the aforementioned topologies is 62 ns, 54 ns and 56 ns accordingly. It was concluded, that average rise time is 283 ns and fall time was 111 ns when commercial driver MBI5026 was used. This is in high contrast with manufacturer specifications. Tamper turn-off produced very short fall time (4.2 ns) but this created large skew in light output response therefore it can be predicted that dimming linearity performance will be the worst. If passive driver is used then rise and fall response are 62 ns and 30 ns correspondingly. Lowest skew was obtained for transconductance amplifier-based topology.**

***Index Terms*—LED dimming, LED display electronics, LED video display, pulse-width-modulation.**

I. INTRODUCTION

Light emitting diodes (LED) are used in both lighting and in the large-scale video displays [1]. In order to maintain the electroluminescence stability (emission wavelength depends on the driving current) LED luminous intensity is regulated using pulse width modulation (PWM) technique [2], [3]. If LED is used in video display, then dynamics of the LED current is important when achieving high accuracy of pixel intensity programming [4]. Aim was to investigate driver topologies influence the dynamics of the LED optical response.

II. RADIANCE INFLUENCE ON PIXEL DIMMING QUALITY

LED luminance can not be controlled by forward current due to current influence on the emission wavelength [5]. Therefore LED video display pixel intensity is controlled by PWM dimming using constant current pulses [6].

The nonlinearity of the human sense of light [7], [8] requires specific approach to light coding. The image capturing equipment mimics the human visual system in order to conserve the stored data amount. This nonlinear correction is addressed as gamma-correction. When image stored in such way is submitted to display it has to be transformed back to linear intensity scale since PWM dimming is inherently linear. This means that the higher number of LED brightness levels is needed for output: large portion of the codes are thrown away in order to obtain the nonlinear radiance response [4].

Conversion of the conventional 8 bit input code C_{in} into gamma-corrected (using ¥ coefficient) code C_{Gamma} with resolution of N bits will exhibit some rounding approximation error [4]

$$¢_{approx} = \left(\frac{C_{Gamma}}{\left(\frac{C_{in}}{255}\right)^{¥} \left(2^{N} - 1\right)} - 1 \right) \cdot 100\% . \qquad (1)$$

For instance, when ¥ is 2.4 only a 19 bit coding resolution is capable of monotonic variance – every change in an input code (8 bits) causes change in an output code within the same direction. This approximation error will increase at the lower end of the coding table.

Several parameters define the LED display quality which sometimes has to be evaluated when display is already assembled [9]. Image refresh frequency has to be above 50 Hz to avoid flicker due to human eye response. If display is used in entertainment, then this frequency should be above 400 Hz in order to avoid flicker caused by scenery video cameras response [10].

All of the above demand very short LED driving current pulses: PWM step granularity so the shortest pulse has to be 38 ns for 400 Hz refresh and 16 bit resolution. ITU recommendation 709 [11] uses a linear slope below the level 8.1 % for gamma correction curve and can be used to relax the dimming resolution requirements down to 14 bits. Then shortest PWM pulse can be just 150 ns. Even in such case LED dimming is prone to driving dynamics caused errors.

Driver response time and LED response time define the shortest attainable PWM pulse duration. It was demonstrated

Manuscript received November 11, 2013; accepted February 18, 2014.

This research was funded by a grant No. 31V-71 from Agency for Science, Innovation and Technology.

in [4] that skew in LED radiation dynamic response, expressed as difference of rising and falling fronts, introduces additional errors in high speed PWM dimming. In case of trapezoidal approximation of pulse fronts error in programmed PWM intensity is proportional to the difference of the rise (t_R) and fall (t_F) fronts of the light output

$$¢_{skewed}\left({}^{2}{}_{on}\right)=\frac{t_F-t_R}{2T}\cdot 100\%. \quad (2)$$

Driver topologies were investigated to evaluate the rise and fall fronts of the light output.

III. LEDS USED IN EXPERIMENTS

LED light is produced by the luminescence [3]. In general it is a solid-state p-n junction diode that gives light output after a forward bias voltage is applied to its terminals. Binary or even ternary semiconductor compounds are used to manufacture LEDs in order to tune the energy gaps. In an electrical sense LED as a load represents a conventional diode. The only difference seen is caused by LED's compound structure: lower forward conduction I-V region steepness due to series resistance and higher leakage current due to shunting path. Widely accepted diode model [12] is presented in Fig. 1.

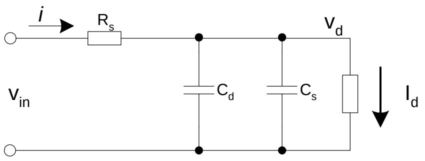

Fig. 1. The forward biased LED equivalent circuit.

It is important to note that series resistance R_s together with capacitance C_s and capacitance C_d in conjunction with nonlinearity of "pure" LED are causing delay in photoluminescence response of the LED and produced light output skew. These capacitances are nonlinear and increase together with forward voltage. LED turn-on response is defined mainly by R_s C_s and C_d which includes the carriers' mobility. LED turn-off time can be much faster since parasitic capacitance is much lower at zero bias voltage and carrier sweep out time can be very short [3]. Therefore it is important to monitor the photoluminescence output when total driver-LED skew is important.

AlGAInP LEDs LO5SMTHR4 from Cotco were used in experiments. Manufacturer specified typical forward voltage was 2.1 V. Measured mean forward voltage was 1.95 V with standard deviation of 0.02 V for lot of 80 devices. Minimum forward voltage was 1.89 V and maximum was 1.98 V. Measured parasitic capacitance was from 20 pF at 0 V bias to 200 pF at 2.1 V forward voltage. Dynamic resistance was 40 Ω at 1 mA down to 7.5 Ω at 20 mA forward current.

IV. DRIVER TOPOLOGIES USED IN INVESTIGATION

LED operating current is 20 mA. All the driver circuits were designed to ensure such forward current during the LED turn-on. Four driver topologies were considered: commercial constant current driver, passive driver, transconductance amplifier and constant current driver with tamper turn-off.

Commercial driver (Fig. 2) MBI5026 [13] supplied by Macroblock was used in investigation. It is an industrial standard widely used in professional video displays [14] and signage. It contains a constant current sink, where current is produced by the current mirror. Turn-off is passive: current sink is disconnected from the output during the off phase.

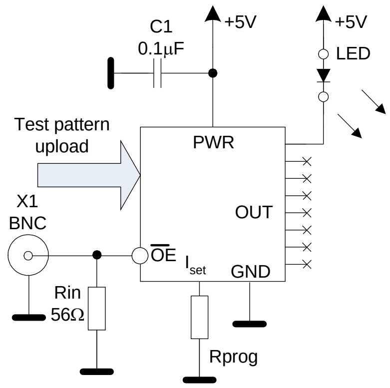

Fig. 2. Commercial LED driver circuit.

Such drivers have relatively slow rise and fall fronts due to limitations of the internal circuitry. Turn on time specified by manufacturer is 40 ns typical and 120 ns maximum value and turn-off time is 70 ns and 200 ns accordingly.

Passive driver used current limiting resistor for driving current programming (Fig. 3).

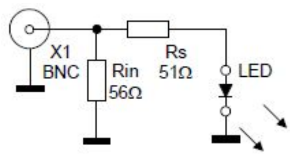

Fig. 3. Passive LED driver circuit.

Operating current was determined by remaining voltage drop on current limiting resistor. Turn-on and turn-off times should be limited only by driving pulses source and time constant formed by current limiting resistor and parasitic LED capacitances. At 200 pF and 7.5 Ω of LED intrinsic resistance plus 76 Ω of the driver circuit this would be 45 ns. Though being simple this circuit has a disadvantage that LED current depends on diode forward voltage drop.

Transconductance amplifier (Fig. 4) was constructed using current feedback amplifier AD8001.

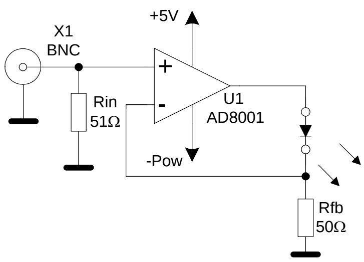

Fig. 4. Transconductance amplifier based LED driver circuit.

This type of amplifier delivers the output current which is proportional to the input voltage [15]. Thanks to fast response of AD8001 it was expected that such driver should deliver shortest rise and fall fronts, approximately 1.5 ns.

Constant current driver (Fig. 5) with tamper turn-off was constructed using passive current source and FDV301N N-channel logic-level MOSFET.

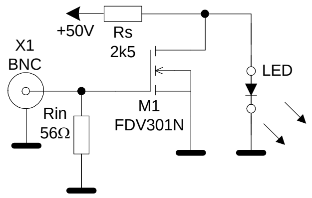

Fig. 5. Constant current LED driver circuit with tamper turn-off.

Current was defined by 50 V bias and 2500 Ω resistor. Such setup ensured that current flowing either through LED of tampering FET was relatively stable (less than 5 %). Expected turn-on delay was 3.5 ns and turn-off delay 6 ns.

V. EXPERIMENT SETUP

Experimental setup is presented in Fig. 6.

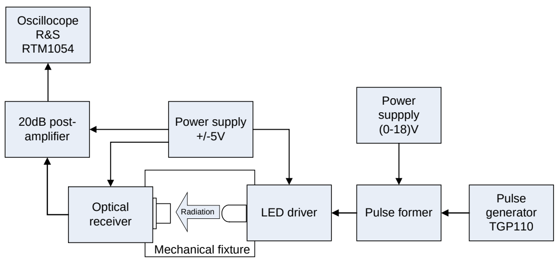

Fig. 6. Experimental setup.

LED driver under investigation was driven by pulse formation circuit designed using ISL55110 driver from Intersil and 50 Ω output resistors. Both positive and negative front durations were 1.5 ns. Formation circuit was fed by pulse generator TGP110 output. Driving pulses were 100 ns or 500 ns long and pulse repetition frequency was 100 Hz to ensure sufficient settling time. Reception of the light pulse was accomplished using transimpedance amplifier (Fig. 7) designed using current feedback amplifier AD8001.

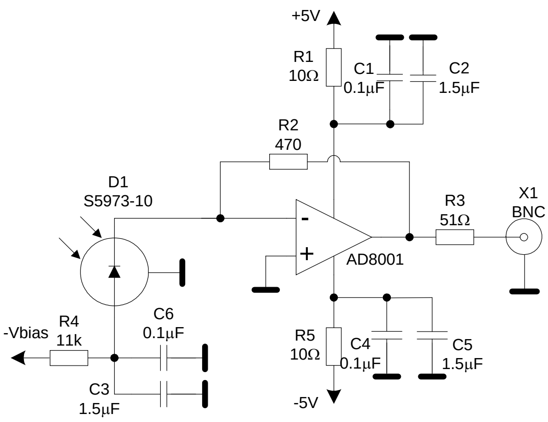

Fig. 7. Transimpedance amplifier circuit used for light pulses' reception.

Receiver circuit speed has been investigated using fast vertical cavity solid state laser transmitter OPV314. Laser and optical receiver were inserted into network analyser ZVL13 for transmission response measurement. Laser was positively biased to enter the lasing mode and then it was used as transmitter of the network analyser output. Optical receiver output was fed into network analyser input. Obtained frequency response (Fig. 8) indicated 270 MHz bandwidth after frequency peak reduction by increasing the feedback resistance.

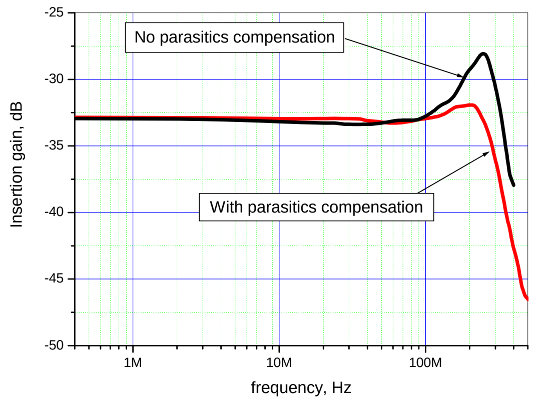

Fig. 8. Small signal transmission response for laser-optical receiver pair.

Receiver was also tested by supplying fast light pulses produced by the same laser driven by passive driver (Fig. 9).

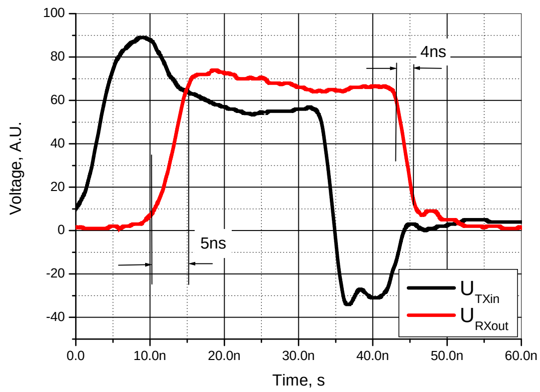

Fig. 9. Receiver response to fast laser pulses.

Measurement indicated rising front t_R duration 5 ns and falling front t_F duration 4 ns at the receiver end. Test results were considered as sufficient proof that receiver speed is sufficient to evaluate the LED light pulses which duration is expected to be tens of nanoseconds.

Same current feedback amplifier AD8001was used as a postamplifier before delivering the signal to 500 MHz bandwidth digital storage oscilloscope DLM2054. Rise and fall front durations t_R and t_F measurement was done using automated measurement feature of the oscilloscope. Every topology was investigated using LO5SMTHR4 LED set of total 85 pieces constructed using several manufacturing lots.

VI. EXPERIMENTAL RESULTS

Rise and fall front measurement results are presented in Fig. 10. Mean values for the measurement are complemented by 3± (standard deviation) to indicate the 99.9 % probability range for the measurement results. It can be seen that LED drivers exhibit different operation speed when in connection with LED. Commercial driver did not produce the specified typical values: instead of specified typical 40 ns and 70 ns for t_R and t_F measurements indicate that 283 ns and 111 ns mean values of light pulses fronts are attained which is far away from specified maximum (120 ns and 200 ns accordingly). Longer response times could be attributed to

LED response influence, but measurements on other topologies indicate that actual LED response time is much faster. Therefore conclusion is drawn that commercial driver did not produced typical response performance and it was at its maximum specified values.

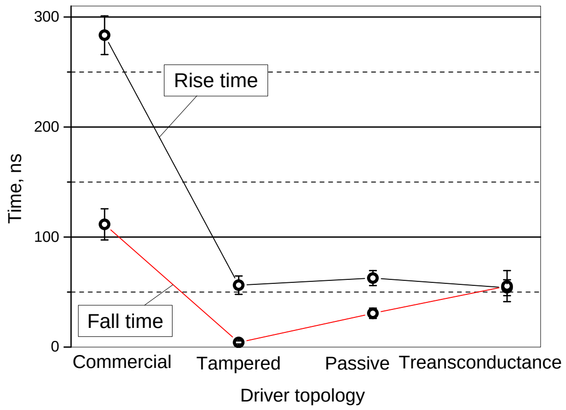

Fig. 10. Rise and fall front measurement results for all topologies.

Passive driver performance is slightly unexpected: despite expected boost in response times it did not perform better than transconductance and tampered constant current counterparts. Measured rise front mean value was 62 ns and turn-off duration was 30 ns. Such asymmetry was expected because LED turn off time could be faster because carriers sweep-out prevails here.

As expected, tamper turn-off topology exhibited shortest response times: tampering the LED ensured fastest light cut-off: 4.2 ns – close to receiver speed (4 ns). Despite such setup seems attractive, it exhibits an asymmetry in pulse response (skew) which in turn will degrade the dimming linearity. Yet, this driver topology indicates the rising front duration (56 ns mean) which can be achieved with almost ideal current source drive.

It must be noted that there was a certain variation in measurement results. This can be seen on two topologies comparison presented in Fig. 11. Whisker diagrams are presented together with data cloud for evaluation of the measurements variation.

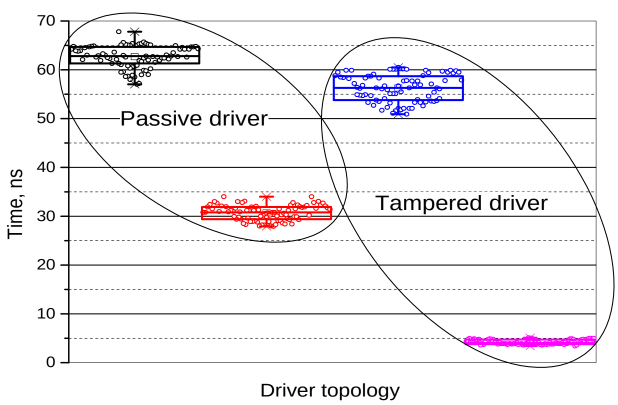

Fig. 11. Rise and fall front data cloud and whisker diagrams for passive and tamper turn-off topologies.

Performance of transconductance topology driver could seem unexpected from the first sight: rise and fall fronts are almost equal despite expected skew (54 ns and 55 ns accordingly). Driver should exhibit skew in driving response since LED is driven by 20 mA/0 mA current pulses and this should cause the light pulse skew, since turn-off is not actively pursued by any current. Nevertheless, this was counterweighted by other phenomena mentioned in chapter III: LED turn-off is much faster due to carrier sweep-out process prevalence in photoluminescence cut-off. This topology must be favoured for LED type investigated since it will induce lowest nonlinearity in dimming response.

VII. CONCLUSIONS

Investigation results indicate that circuits possessing fast constant current drive (passive driver, transconductance amplifier and constant current driver with tamper turn-off) have similar rise time: 62 ns, 54 ns and 56 ns accordingly. It was concluded, that average rise time is 283 ns and fall time was 111 ns when commercial driver was used which is in high contrast with manufacturer specifications. Tamper turn-off produced very short fall time (4.2 ns) but this created large skew in light output response: dimming linearity performance will be the worst. If passive driver is used then rise and fall response are 62 ns and 30 ns correspondingly. Lowest skew and highest dimming linearity was obtained for transconductance amplifier based topology.

REFERENCES

[1] A. N. Motlagh, M. R. Hashemi, M. Hoseinifar, “A novel design for 3-color LED display panel based on CPU processor”, *Journal of display technology*, vol. 7, no. 11, pp. 607–614, 2011. [Online]. Available: http://dx.doi.org/10.1109/JDT.2011.2159191

[2] M. Doshi, R. Zane, “Control of solid-state lamps using a multiphase pulsewidth modulation technique”, *IEEE Trans. power electronics*, vol. 25, no. 7, pp. 1894–1904, 2010. [Online]. Available: http://dx.doi.org/10.1109/TPEL.2010.2043447

[3] E. Shubert, *Light Emitting Diodes*, Cambridge: Cambridge University Press, 2003.

[4] L. Svilainis, “LED PWM dimming linearity investigation”, *Displays*, vol. 29, no. 3, pp. 243–249, 2008. [Online]. Available: http://dx.doi.org/10.1016/j.displa.2007.08.006

[5] A. Zukauskas, M. S. Shur, R. Gaska, *Introduction to solid-state lighting*. Wiley-Interscience. 2002.

[6] H. Ott, L. Plotz, *Dimming InGaN LEDs*. Osram - Opto Semic: Germany, 1999.

[7] C. A. Poynton, “Gamma and its disguises”, *Journal of the Society of Motion Picture and Television Engineers*, vol. 102, no. 12, pp. 1099–1108, 1993.

[8] K. Khursheed, M. Imran, N. Ahmad, M. O’Nils, “Bi-level video codec for machine vision embedded applications”, *Elektronika ir Elektrotechnika (Electronics and Electrical Engineering)*, vol. 19, no 8, pp. 93–96, 2013.

[9] L. Svilainis, “LED directivity measurement in situ”, *Measurement*, vol. 41, no. 6, pp. 647–654, 2008. [Online]. Available: http://dx.doi.org/10.1016/j.measurement.2007.09.003

[10] B. Wendler, *Refresh rate*, Technical note 42, Daktronics Inc., USA, 2002.

[11] *Recommendation ITU-R BT.709*, Basic Parameter Values for the HDTV Standard for the Studio and for International Programme Exchange, Geneva, ITU, 1990.

[12] T. P. Lee, “Effect of junction capacitance on the rise time of LED’s and the turn on delay of injection lasers”, *Bell Syst. Tech. J.*, vol. 54, no.1, pp. 53–68, 1975. [Online]. Available: http://dx.doi.org/ 10.1002/j.1538-7305.1975.tb02825.x

[13] L. Svilainis, “Considerations of the driving electronics of LED video display”, in *Proc. 29th Int. Conf. Information Technology Interfaces*, Cavtat, 2007, pp. 431–436.

[14] Jin-Ho Ahn, “Implementation of an LED tile controller for high-quality image display”, *Displays*, vol. 34, no. 1, pp. 17–26, 2013. [Online]. Available: http://dx.doi.org/10.1016/j.displa.2012.10.004

[15] L. C. Chang, D. S. Lee, P. H. Chen, “A novel LED driving circuits development for decorative lighting system energy saving”, in *Proc. IEEE 4th Int. Microsystems, Packaging, Assembly and Circuits Technology Conf.*, Taipei, 2009, pp. 635–638.